LASER ULTRASOUND: AN INSPECTION TOOL OF SOFT POROUS LOW-DIELECTRIC CONSTANT FILMS FOR MICROELECTRONIC INTERCONNECT*

Colm M. Flannery[1,2,3] and D. C. Hurley[3]

[1]Paul Drude Institute for Solid State Electronics, Berlin, Germany
[2]Colorado School of Mines, Golden CO 80401 USA
[3]National Institute of Standards & Technology, Boulder CO 80305 USA

ABSTRACT The demand for miniaturization in the microelectronics industry requires that the RC (Resistance-Capacitance) factor be lowered to reduce interconnection delay, crosstalk and power loss. The most promising way to achieve this is by introducing porosity into the dielectric film material. We show that laser-generated surface acoustic waves can successfully and rapidly characterize porosity/density and stiffness of these films. Complementary measurements from X-ray reflectivity and Brillouin light scattering verify our results. We discuss why nanoindentation presents difficulties.

INTRODUCTION

Nanoporous aerogel films present perhaps the best candidate for low-dielectric constant (low κ) materials for microelectronic interconnect with reduced RC factor [1,2]. It is becoming increasingly clear that the drastically reduced stiffness properties of porous films limit their introduction for commercial purposes. Thus, a compromise must be reached between low κ value and sufficient mechanical strength (i.e. stiffness) for the material to survive the chemical-mechanical polishing process. There is also a lack of useful and accessible techniques which can accurately provide absolute values of the most important film parameters (density/porosity, Young's modulus E, pore size) suitable for process control. This work reports characterization of density/porosity and Young's modulus of a range of polymer-based nanoporous Methylsilsesquioxane (MSSQ) films via surface acoustic wave spectroscopy (SAWS) which has not previously been applied to such films. The films had porogen concentrations (sacrificial materials used to create pores) of 1 % to 30 %, corresponding to porosities of 14 % to 40 %. Excellent correlations are observed between measured density, porosity and X-ray derived density measurements. The extracted stiffness measurements from Brillouin light scattering (BLS) and SAWS also correlate very well. Nanoindentation, on the other hand, gives stiffness values which are about 3 times the SAWS and BLS values, and we discuss reasons for this. The stiffness dependence on porosity shows that the films are soft (E ~2 GPa) at low porosity, but that, in comparison to silica aerogels, the stiffness properties decrease much more slowly with increasing porosity, so that in the $\kappa<2$ region they may be stronger than the silica aerogel films and therefore may be more suitable for applications. Thus SAWS and BLS represent reliable methods to extract absolute values of critical properties of nanoporous films and reveal unusual strength-porosity behaviour of nanoporous MSSQ.

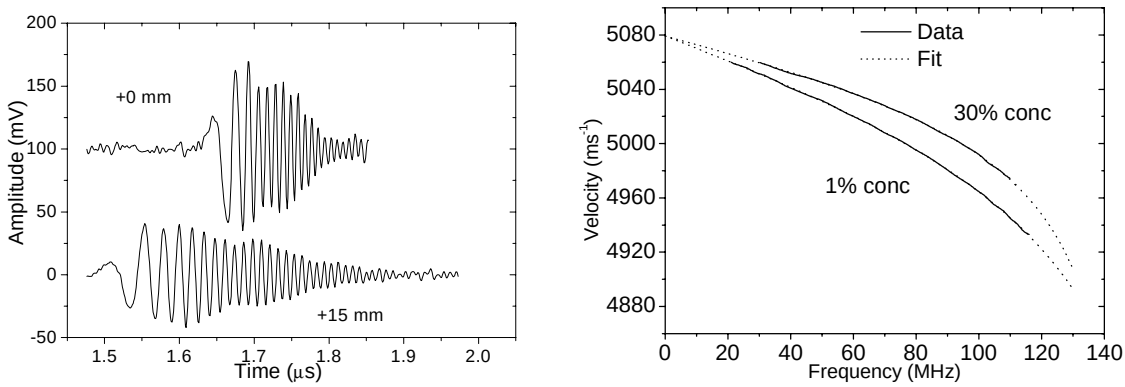

FIGURE 1. (a) Dispersive SAW wavepackets on 1 % sample. (b) dispersion curves for 1 % and 30 % with best fits, from whose parameters the elastic properties are extracted.

EXPERIMENTAL

The samples inspected here were porous MSSQ Zirkon LK™ dielectric films, all 1 μm thick, on Si (001) wafers, with porogen concentrations of 1–30 % [3,4]. Ellipsometric porosimetry has shown a bimodal porosity size distribution (PSD) in the materials; a constant 16 % of the porosity is due to intrinsic micropores (<2 nm diameter), while the porosity increase is due to an increasing number of mesopores, having an almost constant diameter of 3.5 nm (equal to the porogen particle size) over the porosity range measured [3]. MSSQ films are hydrophobic and the matrix has a low κ ~2.7–3. Thus to achieve κ=2, a porosity of ~40 % is needed, whereas ~70 % is required for porous silica films.

In the SAWS technique [5,6], wideband surface acoustic wavepackets are generated thermoelastically from absorption of laser pulse energy at the layer/substrate interface. The laser pulse energy (0.5 mJ, 0.5 ns duration, 337 nm wavelength) is focused into a thin line on the sample (10 μm x 6 mm), causing rapid expansion of the locally heated source, giving rise to stresses and generating surface acoustic wavepackets propagating along the sample. The wideband SAW wavepackets are detected by a piezoelectric foil with steel-wedge transducer at different relative propagation distances (here 15 mm) on the sample. Most of the measurements presented here were obtained with this method, but an alternative optical setup was also used and is discussed below. Figure 1(a) shows a typical SAW wavepacket at different relative propagation distances for a 1 % porogen aerogel film on Si (001). The broadband SAW wavepacket (approx. 20–100 MHz frequency range) propagates in both layer and substrate and becomes dispersed because waves of different frequency sample a different proportion of layer and substrate, with different net elastic properties, and the wave velocity is therefore frequency-dependent. From a Fourier transform technique one extracts the frequency-dependent velocity dispersion curve. Assuming that thickness and Poisson's ratio ν are known, the density ρ and Young's modulus E of the layer are obtained from the best-fit parameters of the theoretical to the measured dispersion curve[5,6]. Figure 1(b) shows measured dispersion curves for the 1 % and 30 % porogen materials together with best fits to the data.

The technique measures absolute values of film properties and is independent of changes in chemical make-up of the film, except in so far as the density or stiffness are altered. SAWS requires propagation lengths of ≈ 10 mm, thus providing mean film values with ≈ 1 minute measurement time.

BLS detects photons inelastically scattered by GHz-frequency range thermal phonons present in the film. Spectra were obtained using a 50 mW, 514 nm wavelength Ar^+ laser. The backscattered light was collected and analyzed by an instrument of the well

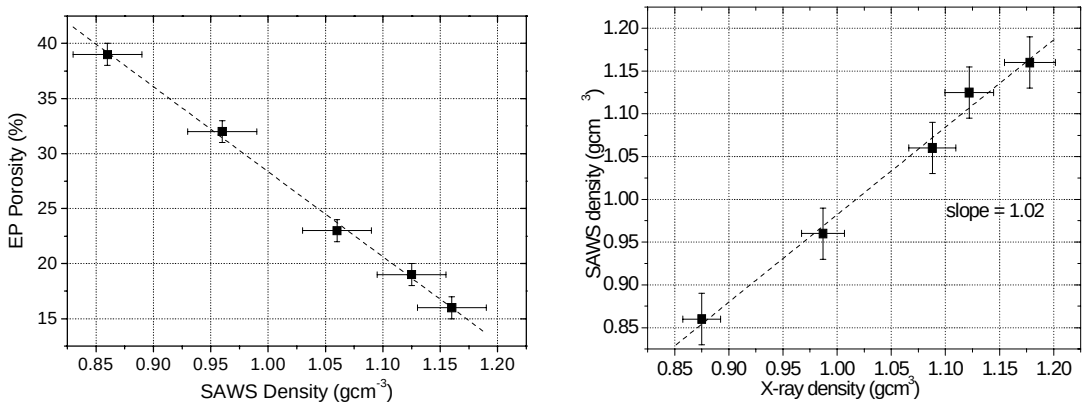

FIGURE 2. (a) Strong linear dependence of porosity on SAWS density. (b) Excellent correlation of SAWS density versus SXR measured density.

known Sandercock-type, 3+3 tandem Fabry-Perot interferometer in the backscattering mode [7]. Both surface acoustic modes and bulk modes may be detected. From measurement of the frequency shift Δf of a peak the velocity V of the corresponding mode is given by; $V=\pi\Delta f/k\sin(\Theta_i)$ for a surface phonon mode; and $V=\pi\Delta f/kn$ for a bulk phonon mode, where Θ_i is the light incidence angle, k is the absolute value of the laser light wavevector, and n is the refractive index of the material.

Complementary data was supplied by ellipsometric porosimetry (EP) (pore size and distribution, film thickness and refractive index) [8], specular X-ray reflectivity (SXR) (film density) [9] and Nanoindentation (NI) [10].The BLS values of E were derived from measurement of the film bulk longitudinal velocity combined with a BLS-measured Poisson's ratio of 0.26 for the 1 % sample.

RESULTS AND DISCUSSION

Complementary measurements

Figure 2(a) plots EP porosity as a function of SAWS density. A strong linear dependence is clear. Comparing the SAWS density to the SXR density (Figure 2(b)) yields a linear fit with almost ideal slope of 1.02 ± 0.06. The SAWS technique clearly provides reliable density values with remarkably strong correlations between porogen concentration, porosity and density. We can calculate a skeletal density of ~1.4 g/cm^3, typical for bulk MSSQ.

All-optical SAWS measurements

A major disadvantage of the piezoelectric foil detector technique is that it requires contact to the sample surface. This is clearly undesirable for rapid measurement and for in-situ inspection applications. An optical probe does not present this problem. In addition, an optical point-probe detector has the potential to detect up to higher frequency than a line-shaped transducer. To this end, we have used a Michelson interferometer laser ultrasound setup [11], to carry out benchmarking measurements on porous polymer films.

This instrument is based on SAW generation by a 200 ps duration, 532 nm wavelength frequency-doubled pulsed YAG laser and detection with a 1064 nm wavelength probe laser configured in a Michelson interferometer setup. When the generated SAW wavepacket passes under the probe beam, the optical path length is altered,

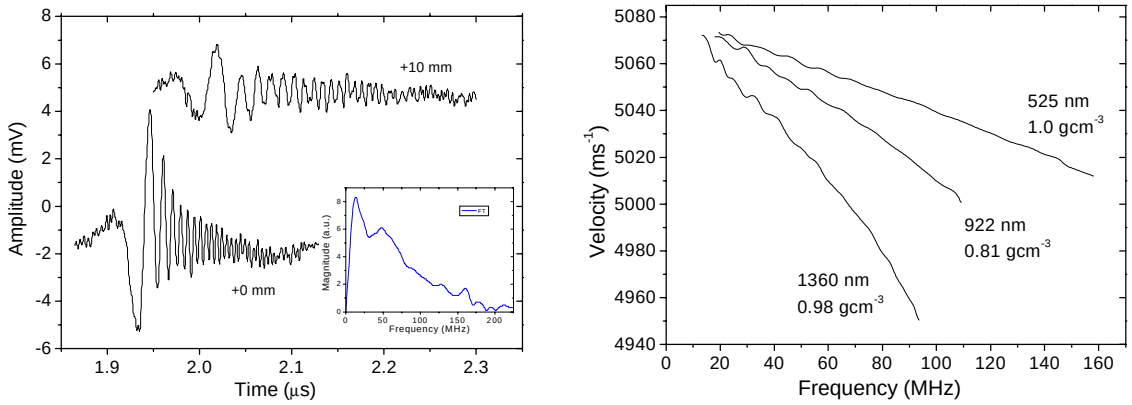

FIGURE 3. Optically detected data (a) Surface acoustic wavepackets on 666 nm SiLK on Si, detected (b) Frequency-dependent velocity dispersion curves for MSSQ films of varying thickness and porosity.

causing a change in the detected light intensity at the optical receiver. Because the 1064 nm wavelength penetrates into silicon we inspected only samples on highly-doped silicon wafers that reflected light from the substrate surface. These samples were three MSSQ samples of similar matrix material but varying porosity and two low-κ polymers, Dow Chemical SiLK™ (an aromatic polymer) and Dow Corning XLK™ (a hydrogen silsesquioxane), all of great commercial interest.

Figure 3(a) shows optically-detected SAW wavepackets on the SiLK sample. The wavepackets are similar in form to Figure 1(a) although the signal-to-noise ratio (SNR) is not as good. Dispersion curves were extracted from the waveforms by the same Fourier transform technique and Figure 3(b) shows these curves for three MSSQ samples. One sees that the level of dispersion depends on the film thickness, and that the curves are similar in shape to Figure 1(b), but with a certain amount of waviness in the low-frequency region, due to poorer SNR. Extracted elastic parameters from these optical measurements are given in Table 1, together with parameters extracted from piezoelectric foil measurements. The

TABLE 1. Measured properties of 5 porous thin film samples inspected by PDI, Germany (piezoelectric foil) and NIST (optical). E (GPa), ρ (gcm^{-3}), d thickness (nm)

		Piezelectric foil		*Optical*	
Sample	d (nm)	ρ	E	ρ	E
MSSQ	1360	0.97	1.7	0.98	2.2
MSSQ	922	0.79	0.93	0.81	0.99
MSSQ	525	0.91	1.5	0.99	1.9
SiLK™	632	0.96	2.2	1.0	3.0
XLK™	502	0.90	1.3	0.96	2.4

values of density and Young's modulus are comparable. Density values are very close indeed, especially for the thicker films which provide more dispersion and hence better quality fit. Typical density errors for SAWS measurements are 1-2 %. For Young's modulus, which is more sensitive to quality of fit, typical errors are 20 %. Thus the extracted E values are comparable between the two methods. These measurements are a preliminary investigation of different SAW techniques. Based on these results we are designing an optimized system, working at laser wavelengths convenient for silicon, that can automatically carry out SAWS measurements and analysis, and should provide results with much better SNR and quality of fit. It is worth pointing out that in coming years materials with increasingly lower κ will be introduced: these will have lower density

(higher porosity). Inspection methods such as X-ray and ellipsometry become less sensitive as density decreases. However, SAWS sensitivity derives from the impedance mismatch between substrate and layer. New materials will have a greater impedance mismatch. This means that SAWS will become even more suitable as an inspection tool in the future and competing methods less so.

BLS measurements

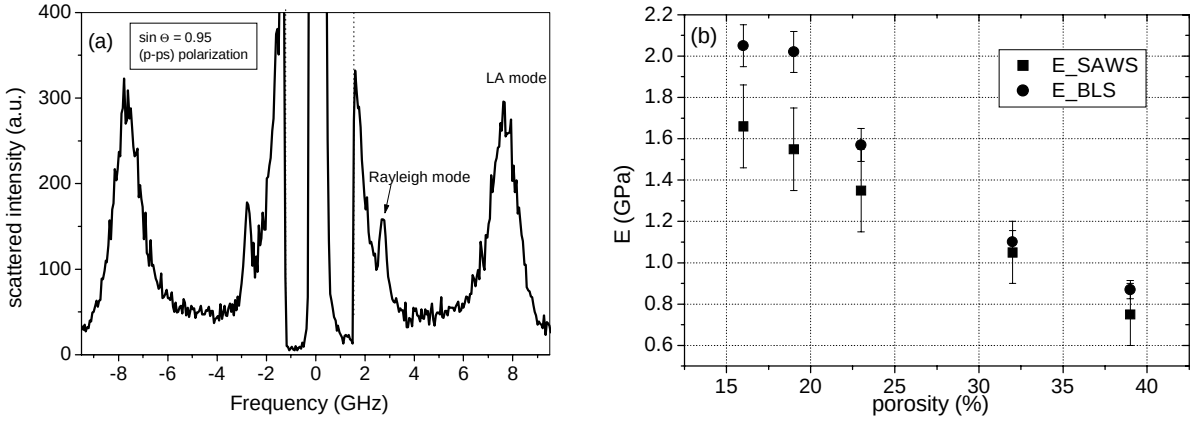

FIGURE 4. (a) BLS spectrum from 1 % porogen MSSQ film showing Rayleigh and Longitudinal peaks. (b) Young's modulus, E derived from BLS and SAWS as a function of porosity.

A BLS spectrum of the 1% porogen sample is shown in Figure 4(a). Peaks due to a bulk longitudinal mode and a Rayleigh mode are detectable. Angular dispersion of the longitudinal mode peak revealed the films to be essentially elastically isotropic. The Rayleigh mode was not detectable on the samples > 5 % porogen concentration. We could determine a surface wave velocity of 770 ± 5 ms^{-1} for the 1 % sample. With the determined longitudinal mode velocity $V_l = 1458$ ms^{-1}, this gives a Poisson's ratio $\nu = 0.26 \pm 0.01$. This is the first time Poisson's ratio has been accurately determined for such a nanoporous thin film. Assuming that ν changes little with density, the Young's modulus is obtained from $E = \rho V_l^2(1+\nu)(1-2\nu)/(1-\nu)$ for the different ρ and V_l values measured on each film.

Fig. 4(b) plots the BLS E values and SAWS E values as a function of porosity. The values from both techniques are, at most, ≈ 20 % different. Considering that the BLS E values are derived at ≈ 8 GHz from longitudinal mode, and the SAWS values at ≈ 100 MHz from a primarily transverse mode this can be considered an excellent mutual verification of the E values extracted from both techniques; again showing that SAWS provides reliable values. Recent EP measurements allow Young's modulus to be derived from expansion and contraction of the film with gas adsorption and yield very similar values of E [12]. A thermal grating method [13] also provides similar values to SAWS.

From the peakwidth of the longitudinal mode we obtain the attenuation, which is expected to increase with porosity. The attenuation does indeed increase up to 23% porosity but levels off above this [4]. This might be attributable to the bimodal PSD of these materials [3]. Above 23% the porosity is dominated by the larger pores and the attenuation/scattering is dominated by the effects of these pores, with different attenuation rate. This might also signal the onset of pore interconnectivity with a consequently different scattering mechanism. This is a very interesting behaviour which we are now investigating in more depth for a wider range of films.

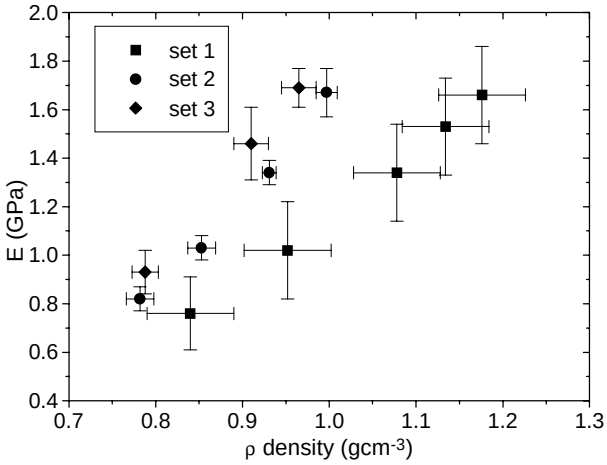

FIGURE 5. SAWS-measured stiffness-density dependence for three MSSQ sample sets. The stiffer sets have larger stiffness decline (slope) as density decreases.

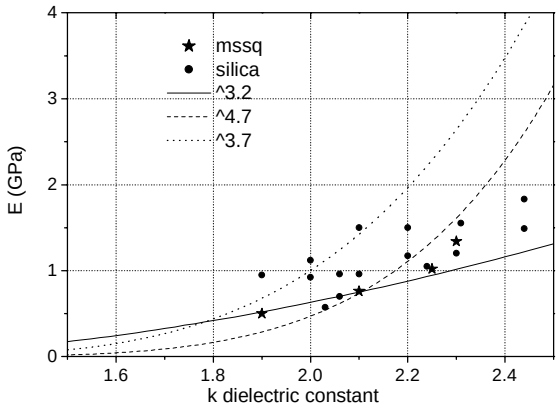

FIGURE 6. Modeled power law dependence of Young's modulus on dielectric constant for porous silica and MSSQ materials, compared to measured data.

Stiffness-density dependence

The stiffness dependence of the MSSQ films on density is shown in Figure 5 (set 1), as well as data for MSSQ samples from two other manufacturers (sets 2 and 3). One sees that the stiffness reduces in a consistent way with decreasing density (increasing porosity) for each set. Each set has manufacturer-specific formulations and processing routes and shows clear differences in matrix stiffness at similar densities. It is interesting to note that the stiffer-matrix materials decline more rapidly (have a larger slope) as density decreases. Extrapolation indicates that at lower densities the softer-matrix material (set 1) might have higher stiffness. These MSSQ films are initially soft (~2.2 GPa) but decline slowly whereas silica films are initially stiff (74 GPa) but decline drastically in stiffness [1]. This MSSQ strength behaviour can be attributed to the small and constant pore size, ensuring that the matrix is still well-interlinked as porosity increases. Figure 6 shows the modeled stiffness dependence of set 1 as a function of κ compared to that for silica aerogel (κ was modelled by a Bruggeman effective-medium approximation for both materials, E by a power-law dependence on density $E \sim \rho^n$). Also plotted for comparison are measured κ and E values for the materials. In the region of $\kappa=2$ the stiffnesses are quite similar. If one extrapolates to $\kappa<2$, then the figure indicates that the MSSQ films have higher stiffness.

Nanoindentation

Nanoindentation (NI) is the most common method for obtaining stiffness of thin films [10]. However the analysis of data for the case for soft, thin (= 1 μm) film on a stiff substrate is much more complicated than the stiff-on-soft case. E values from NI and SAWS for the different porogen concentration MSSQ films are shown in Figure 7. While the results are similar in form, stiffness declines with porogen concentration, the magnitudes of the results from the two techniques are not compatible. NI consistently gives a value of E about 3 times greater than that from SAWS or BLS. We have also observed similar NI-SAWS

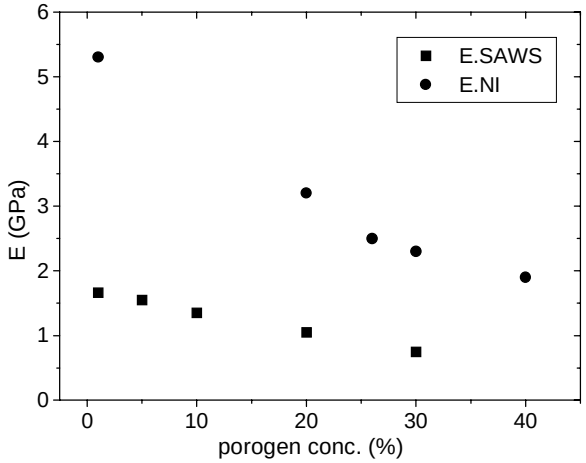

FIGURE 7. Comparison of E, Young's modulus as a function of porogen concentration measured from SAWS and Nanoindentation. NI values are about 3 times larger.

relationships for porous silica films [14]. There are several reasons why NI may overestimate stiffness: (a) Stiffening by the substrate. For such thin films the NI tip may always feel the effect of the substrate stiffness and thus overestimate E; (b) Viscoelasticity. Polymers are known to show large viscoelastic effects which are likely to cause higher E values to be obtained [15]; (c) Tip-film interactions. Effects such as densification or pile-up under the tip have not been quantified. Additionally the interactions of a tip with such a porous matrix are not understood. NI is certainly a useful technique for such films, especially for purposes of comparison between similar films of similar thicknesses. But we believe that more measurement and analysis care is needed: penetration depth and force should both be very small, and automated measurement methods developed for hard films should not be used. At the present time we recommend that absolute stiffness values provided by NI be treated with 'a grain of salt'.

CONCLUSIONS

Surface acoustic wave spectroscopy has been applied to a matrix of nanoporous polymer films for low-κ dielectric application. SAWS-derived density correlates excellently with X-ray measurements, and the strong correlation between Young's moduli from both BLS and SAWS indicates that the extracted values are reliable. Strong correlations are also present between values of density, porosity and stiffness. Benchmarking measurements made with an all-optical Michelson interferometer detection setup show that both SAWS setups provide comparable results, the optical technique having the advantage of being non-contact. Nanoindentation measurements provide stiffness values about 3 times higher than SAWS and BLS. We believe that this is due to a combination of data analysis effects,

viscoelasticity, substrate stiffening and unquantified tip-film interactions. The porosity-stiffness dependence shows that the stiffness decreases strongly with increasing porosity, but that this rate of decrease also depends on the manufacturer-specific properties of the matrix. The stiffer-matrix material tends to decrease more sharply as porosity increases. The softer MSSQ material shows a slower decrease in stiffness with porosity, which means that in the $\kappa<2$ region it might have better stiffness properties than materials which have higher stiffness at higher κ. The SAWS technique is nondestructive, relatively inexpensive, and has the potential to provide absolute values of material properties more accurately than other techniques. The experiments described here indicate how SAWS may be a valuable process control tool to develop and standardise nanoporous film properties.

ACKNOWLEDGEMENTS

We acknowledge the partial support of EU project EFRE (C.F), M.R. Baklanov, XPEQT at IMEC, Belgium for EP measurements, T. Wittkowski, K. Jung and B. Hillebrands, University of Kaiserslautern, Germany for BLS measurements, and M. Gallagher of Shipley for sample supply.

REFERENCES

1. C. Jin, J.D. Luttmer, D.M. Smith, T.A. Ramos, *MRS Bull.* **22** (10) 39 (1997).
2. C.J. Hawker, J.L. Hedrick, R.D. Miller, W. Volksen, *MRS Bull.* **25** (4), 54 (2000).
3. M.R. Baklanov, C. Jehoul, C.M. Flannery et al, *Proc. 2001 MRS Advanced Metallisation Conference (AMC)*, Montreal, Canada.
4. C.M. Flannery, T. Wittkowski, K. Jung, B. Hillebrands, M.R. Baklanov, *Applied Physics Letters* **80** 4594, (2002)
5. R. Kuschnereit, H. Fath, A.A. Kolomenskii, M. Szabadi, P. Hess, *Appl. Phys. A* **61,** 269 (1995).
6. C.M. Flannery, C. Murray, I. Streiter, S.E. Schulz, *Thin Solid Films* **588**, 1-4 (2001).
7. B. Hillebrands, Rev. Sci. Instrum. **70**, 1589 (1999).
8. M.R. Baklanov, K.P. Mogilnikov, V.G. Polovinkin and F.N. Dultsev, *J. Vac. Sci. Technol. B* **18**, 1385 (2000).
9. W.-L. Wu, W. E. Wallace, E.K. Lin, G.W. Lynn, C.J. Glinka, E.T. Ryan, H.-M. Ho, *J. Appl. Phys.* **87**, 1193 (2000).
10. J.L. Hay, G.M. Pharr, in *ASM Handbook Vol. 8: Mechanical Testing and Evaluation*, ed. H. Kuhn and D. Medlin, (ASM International, 2000), pp. 232-243.
11. D.C. Hurley, V.K. Tewary and A.J. Richards, *Meas. Sci. Technol.* **12** 1486 (2001)
12. K.P. Mogilnikov and M.R. Baklanov, "Determination of Young modulus of porous low-K films by ellipsometric porosimetry", submitted to *Electrochem. Sol. St. Lett.* (2002)
13. D. Nelsen, M. Gostein, A.A. Maznev, Proc. 9th. Symp. on Polymers for Microelectronics, Wilmington, Delaware, May 2000.
14. C.M. Flannery, C. Murray, I. Streiter, S.E. Schulz, M.R. Baklanov, MRS Proc. 714E, 2001.
15. M.R. VanLandingham, J.S. Villarrubia, W.F. Guthrie, G.F. Meyers, *Macromolecular Symposia* **167**, 15-44 (2001).

Any mention of commercial products is for information only; it does not imply recommendation or endorsement by the National Institute of Standards and Technology nor does it imply that any products mentioned are necessarily the best available for the purpose.